Analytical and Bioanalytical Chemistry (2019) 411:6275–6285
https://doi.org/10.1007/s00216-019-01578-8

RESEARCH PAPER

Detection and fragmentation of doubly charged peptide ions in MALDI-Q-TOF-MS by ion mobility spectrometry for improved protein identification

Jens Sproß[1] · Alexander Muck[2] · Harald Gröger[1]

Received: 8 October 2018 / Revised: 22 November 2018 / Accepted: 4 January 2019 / Published online: 13 March 2019

Abstract

Today, bottom-up protein identification in MALDI-MS is based on employing singly charged peptide ions, which are predominantly formed in the ionization process. However, peptide mass fingerprinting (PMF) with subsequent tandem MS confirmation using these peptide ions is often hampered due to the lower quality of fragment ion mass spectra caused by the higher collision energy necessary for fragmenting singly protonated peptides. Accordingly, peptide ions of higher charge states would be of high interest for analytical purposes, but they are usually not detected in MALDI-MS experiments as they overlap with singly charged matrix clusters and peptide ions. However, when utilizing ion mobility spectrometry (IMS), doubly charged peptide ions can be actively used by separating them from the singly protonated peptides, visualized, and selectively targeted for tandem MS experiments. The generated peptide fragment ion spectra can be used for a more confident protein identification using PMF with tandem MS confirmation, as most doubly protonated peptide ions yield fragment ion mass spectra of higher quality compared to tandem mass spectra of the corresponding singly protonated precursor ions. Mascot protein scores can be increased by approximately 50% when using tandem mass spectra of doubly charged peptide ions, with ion scores up to six times higher compared with ion scores of tandem mass spectra from singly charged precursors.

Keywords Doubly charged peptide ions · Ion mobility spectrometry (IMS) · MALDI-Q-TOF mass spectrometry · Protein analysis · Proteomics

Introduction

In recent decades, mass spectrometry has emerged as the dominating analytical method for unraveling the sequences of proteins. The impressive achievements in the field of proteomics would not have been possible without this analytical tool [1, 2]. Today, *bottom-up* protein identification is the preferred mass spectrometry methodology either performed by *on-line* liquid chromatography–electrospray ionization mass spectrometry (LC-ESI-MS) or matrix-assisted laser desorption ionization–mass spectrometry (MALDI-MS) [3, 4]. While mainly multiply charged peptide ions are used for protein identification in LC-ESI-MS, MALDI-MS protein identification is based on singly protonated peptide ions as MALDI mainly generates such singly charged ions [5].

At the same time, multiply charged ions in MALDI are not unknown and when analyzing intact proteins, doubly charged protein ions are commonly observed. Depending on the size of the protein chain, even higher charge states have been reported, although the singly charged protein ion has usually the highest intensity [6–8]. MALDI using IR lasers employing glycerol as a liquid matrix has been also reported to yield multiply charged protein ions [9–11]. Similar results were obtained when analyzing peptides using glycerol as matrix and IR lasers [12, 13] or glycerol as addition to matrix solutions and

Published in the topical collection *Close-Up of Current Developments in Ion Mobility Spectrometry* with guest editor Gérard Hopfgartner.

Electronic supplementary material The online version of this article (https://doi.org/10.1007/s00216-019-01578-8) contains supplementary material, which is available to authorized users.

✉ Jens Sproß
j.spross@uni-bielefeld.de

✉ Harald Gröger
harald.groeger@uni-bielefeld.de

[1] Industrial Organic Chemistry and Biotechnology, Faculty of Chemistry, Bielefeld University, Universitätsstr. 25, 33615 Bielefeld, Germany

[2] Waters GmbH, Helfmann-Park 10, 65760 Eschborn, Germany

UV lasers [14], respectively. A commercially available MALDI mass spectrometer is usually equipped with a UV laser. Therefore, improving the performance of UV-MALDI-MS by the introduction of novel matrices has been of strong interest. Jaskolla et al. presented α-cyano-4-chlorocinnamic acid (Cl-CCA) as rationally designed MALDI matrix which enabled lower detection limits compared with α-cyano-4-hydroxycinnamic acid (CHCA) [15, 16]. They also reported the detection of strong doubly charged peptide ions when they investigated this matrix compound [16]. However, the novel halogenated matrices can only be used with UV lasers with wavelengths < 355 nm as the absorption of these compounds at higher wavelengths is significantly lower. As many state-of-the-art mass spectrometers are equipped with solid-state lasers, operating at 355 nm, only low signal intensities are obtained [17, 18]. Cramer et al. investigated the fragmentation behavior of doubly charged peptide ions generated in UV-MALDI [19]. The most intense doubly charged peptide ions were detected with 2,5-dihydroxybenzoic acid (DHB) as a matrix. They also reported that the fragmentation behavior of multiply charged ions was not dependent of the ionization process—doubly charged ions generated in MALDI and ESI yielded similar tandem mass spectra.

Despite all these recent findings, doubly charged peptide ions in MALDI are not used for the identification of proteins, due to further practical limitations, such as low intensity of multiply charged peptides in most MALDI spectra relative to singly charged ions (making automatic triggering of dependent scans difficult, if not impossible), or for other reasons, such as overlapping peaks of matrix clusters. Alternative approaches would have a huge potential for improving protein identification in MALDI-TOF tandem MS experiments.

The major hurdle results from the fact that singly charged ions are predominantly formed in the MALDI ionization process; doubly charged peptide ions are either detected with low intensities and signal-to-noise ratios [16, 19] or not detected in the mass spectra. This is not the case for singly charged peptide ions stemming from the widespread tryptic hydrolysis protocol, as they are populating a higher *m/z* range, starting above approximately *m/z* 800. A major aspect of the typical route utilizing singly protonated peptide precursors in MALDI is their lower fragmentation efficiency. Tryptic peptides carry their first adduct proton usually on the basic *C*-terminus (either K or R). This fact has adverse effects on fragmentation statistics known from the "mobile proton model", namely in detail a lower amount of fragment ions [20]. CID fragmentation of a singly charged precursor ion always leads to the formation of an even electron fragment cation and a neutral loss counterpart. This might result in lower frequency of appearance of complete fragment ion series and correspondingly lower scoring values in database searches. Moreover, the fragmentation is typically carried out at higher collision energies causing higher levels of noise and overfragmentation. Due to this overall lower spectral quality compared to fragment ion mass spectra obtained from doubly or triply charged peptide ions, there is a need for new analytical approaches.

With ion mobility spectrometry (IMS) it is possible to separate ions based on their gas phase behavior (depending on the shape and thereby also on the mass of the molecule [21] and charge state [22]). Using IMS, protein structures can be elucidated [23], structural isomers of carbohydrates can be differentiated [24, 25], and isobaric peptides can be separated and individually fragmented [26–28]. Therefore, IMS is the method of choice for the selection of doubly charged peptide ions in MALDI-MS.

In the following sections, we report an ion mobility–enabled selection of multiply charged ions for MALDI-TOF tandem MS proteomic analysis. We made use of a hybrid Q-TW-IMS-*oa*-TOF mass spectrometer [29]. Sample preparation is comparable to the peptide mass fingerprinting (PMF) approach for the analysis of proteins [30, 31]. Protein samples were analyzed after tryptic digestion. This methodology provided an effective tool to obtain fragment mass spectra of doubly charged peptide ions and enabled the identification of proteins with higher confidence compared with the approach based on singly charged peptide ions routinely used in MALDI experiments. This approach allows a straightforward selection of doubly charged peptide ions for protein identification by PFF and is not dependent on special matrix compounds but makes use of the well-established matrix DHB. This compound is well known and commercially available. To our knowledge, this is the first systematic approach comparing the identification efficiency of the two ion types in MALDI peptide analysis. We further demonstrate that this approach also contributes to an improved protein identification by database search using MALDI tandem MS data since higher scoring values were obtained when using fragment ion spectra of doubly charged peptide ions compared with fragment ion spectra obtained from the corresponding singly charged peptide ions.

Methods

Sample preparation

MassPrep™ tryptic enolase digest (enolase I from *Saccharomyces cerevisiae*, SwissProt P00924) was purchased from Waters (Milford, MA, USA). Ene reductase from *Gluconobacter oxydans* was kindly provided by the group of Prof. Werner Hummel and recombinantly expressed as published recently [32]. The reduced and alkylated (iodoacetamide) protein was digested *in-solution* with 1:20 wt/wt trypsin gold (Promega, Madison, WI, USA) overnight. The peptide mixture was desalted using C18-Ziptips (Millipore, Milford, MA, USA) according to

the protocol suggested by the manufacturer and dried in a SpeedVac. Compositions of the matrix solutions can be found in detail in the Electronic Supplementary Material (ESM, Table S2) The protein digests were reconstituted in water, 3% ACN, and 0.1% trifluoroacetic acid and were spotted onto a stainless steel target plate with the matrix solutions (0.5 μL/0.5 μL; 250 fmol on spot) using the dried droplet method.

Mass spectrometry and ion mobility spectrometry

In our experiments, a hybrid Q-IMS-oa-TOF mass spectrometer (Synapt G2Si, Waters Corp., Manchester, UK) equipped with a medium pressure MALDI ionization source and a travelling wave ion mobility spectrometry (TW-IMS) cell has been employed. Mass spectra were recorded in a mass range of *m/z* 350–3500. The instrument used a 1000-Hz Nd:YAG laser with a wavelength of 355 nm and a focus set to approximately 60 μm diameter. The laser had a pulse time of 2 ns and a tunable repetition rate (200–2500 Hz, operated at 500 Hz) with laser energy ~ 30 μJ/pulse/1 kHz. The laser energy was set to 50% when CHCA was used as matrix and 72% for the other matrix compounds. The source voltage settings were as follows: sample plate 0 V, extraction voltage 10 V, hexapole bias 10 V, and aperture 0 set at 0 V. Trap collision cell voltage used 4 V and a flow of 2 mL/min of argon; the transfer collision cell was at 2 V. The helium cell prior IMS was set at 180 mL/min and the IMS occurred at 80 mL/min of nitrogen. The data were collected in MassLynx™ 4.1 software. The pressure on the sample plate was regulated by setting a flow of cooling nitrogen gas through the source block (0–100 mL/min). The optimal cooling gas flow was approximately 100 mL/min which resulted in MALDI sample plate pressure of 0.5 mbar. Calibration of the instrument was performed using red phosphorus, as recently reported [33]. MALDI-Q-IMS-TOF mass spectra were recorded in the sensitivity mode at a trap DC bias of 45 V.

Tandem MS experiments

In a second step, fragmentation of peptide ions was performed using CID. The isolation window of the quadrupole was 4 Da wide; the collision gas was argon. The collision energy was tuned manually (see ESM Tables S4 and S6). For tandem MS experiments in the TOF mode, the trap collision cell was used; for fragmentation in the IMS mode, the transfer collision cell (behind the IMS separation cell, compare ESM Fig. S5) was used.

Data analysis and processing

Data analysis and processing were performed using MassLynx™ 4.1, Driftscope™ v2.9, and BioLynx™ (Waters Corp., Manchester, UK). For database searches using an *in-house* Mascot server, mass spectra were deconvoluted and deisotoped using MaxEnt3 and exported in the Sequest text file format. For database searches of tandem MS data, a "multiple pkl" format was used (i.e., fragment spectra of several precursor ions are combined in a single searchable .pkl text file). For enolase, the SwissProt database was used. For ene reductase from *G. oxydans*, a database containing the reviewed protein entries of *Gluconobacter oxydans* from the UniProt database was generated and the sequence of the *N*-terminally his-tagged ene reductase from *G. oxydans* was added.

Results and discussion

IMS tuning for optimal resolution

A tryptic enolase digest at 250 fmol on target was used as standard sample throughout all experiments. Without the use of IMS, the obtained MALDI mass spectra were dominated by singly charged peptide ions (Fig. 1A1–3). Using TW-IMS, however, we were able to visualize doubly charged peptide ions generated during the ionization process (Fig. 1B1–3). For the optimization of the ion mobility separation, the enolase digest was spotted on the target using CHCA as matrix (M1, ESM Table S2) and data was acquired in the mobility mode. The mobilograms of the doubly charged ions of the tryptic peptides at *m/z* 895.42 (sequence: AAQDSFAAGWGVMVSHR) and *m/z* 920.96 (sequence: SIVPSGASTGVHEALEMR) were compared at different wave velocity gradients (ESM Table S1). The wave height of the TW-IMS remained unchanged at 40 V. The optimal wave velocity gradient setting was found to be 1200–400 m/s. A resolution of the two peaks of $R = 0.84$ and a peak capacity of 53 for the peptide ion at *m/z* 895.42 (ESM Table S1) were achieved. These settings were used during the following experiments.

Matrix screening

Using optimized IMS settings, different matrix compounds and formulations (ESM Table S2) were screened for the most abundant formation of doubly charged peptide ions. These matrix formulations included the commonly used matrix CHCA, the rationally designed matrix Cl-CCA, the structurally related matrix α-cyano-4-fluorocinnamic acid (F-CCA), a mixture of Cl-CCA and α-cyano-2,4-difluorocinnamic acid (DiF-CCA), and DHB, the last one being mostly used for the analysis of proteins. The mass spectra were evaluated using signals of four peptide ions, detected both in TOF and IMS modes (ESM Table S3). We were able to detect doubly charged peptide ions using all matrix formulations. The signal intensities, signal-to-noise ratios, and *m/z* ratios of

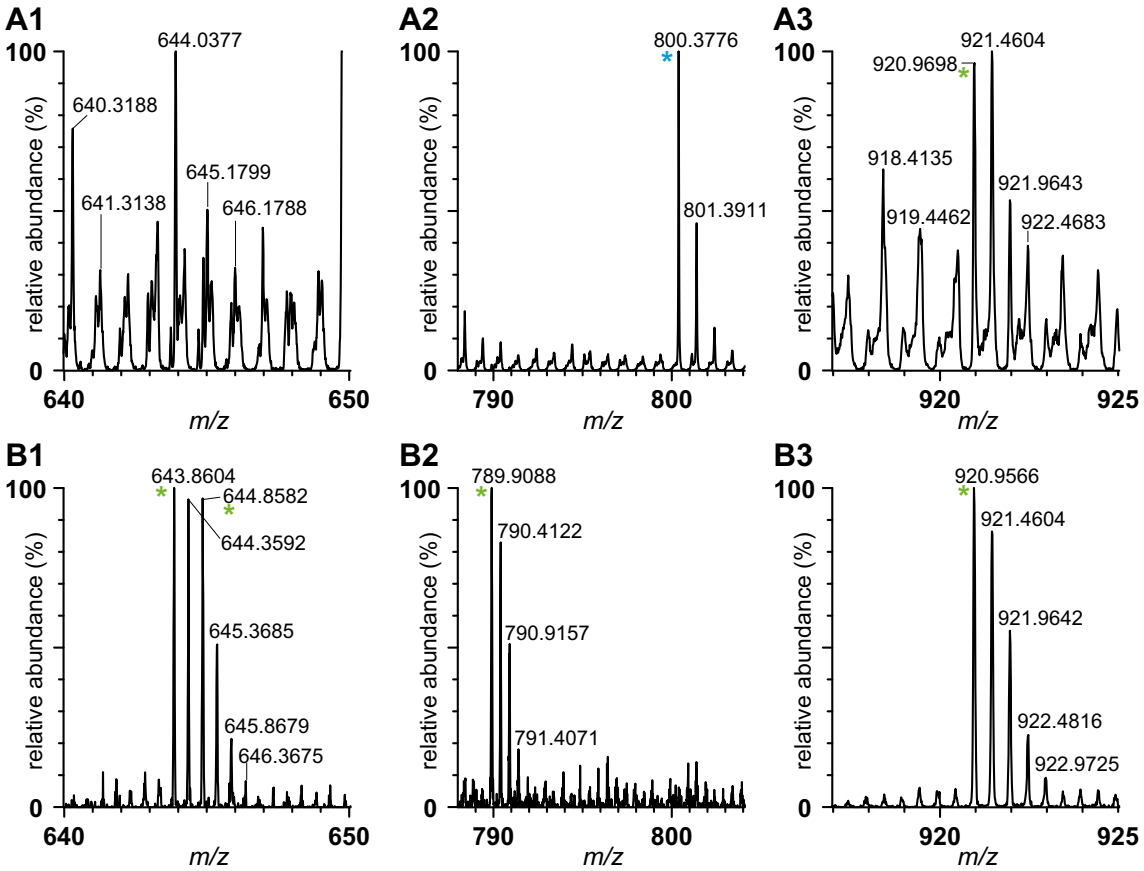

Fig. 1 **A1–3** Mass spectra acquired by MALDI-Q-TOF-MS (matrix, CHCA, M1). The spectra are dominated by singly charged ions (compare also Fig. 2). **A2** Singly charged peptide ion at *m/z* 800.38, assigned to yeast enolase I peptide (sequence YDLDFK, amino acids 259-264) by PMF. **A3** With a low signal-to-noise ratio, a doubly charged ion is detected and assigned to yeast enolase I (*m/z* 920.96, sequence SIVPSGASTGVHEALEMR, amino acids 33-50; compare ESM Table S4). **B1–3** TW-IMS enables the separation of ions based on their charge states. This makes doubly charged ions, generated in the MALDI process, visible which are ordinarily overlaid by the more intense singly charged ions. The ions with green asterisks are assigned to yeast enolase I by PMF. **B1** *m/z* 643.86, sequence NVNDVIAPAFVK, amino acids 68-79 and *m/z* 644.86, sequence VNQIGTLSESIK, amino acids 347-358; compare ESM Table S4) **B2** *m/z* 789.91, sequence AVDDFLISLDGTANK (amino acids 89-103) **B3** *m/z* 920.96, compare to **A3**

the peptides were strongly dependent on the matrix formulation (compare ESM for further details). The performance of the matrix CHCA was good; however, doubly charged peptides were mainly detected below *m/z* 1350 in the IMS mode (ESM Fig. S3). Using the halogenated matrices, signal intensities of the mass spectra were considerably lower compared with those of the mass spectra obtained with CHCA. The reason for these results is most likely the low absorbance of the matrix substances at the wavelength of the MALDI laser [15, 17]. The matrix DHB outperformed the other matrices tested in this study, and the spectral intensities were dependent on the DHB concentration. At the commonly employed concentration of 130 mM DHB (corresponding to 20 mg/mL; M6a-c, ESM Table S2), the mass spectra were similar to the mass spectra obtained using CHCA but with a signal intensity at least one order of magnitude lower (ESM Figs. S1 and S2).

When the concentration of DHB was raised to 1.3 M (corresponding to 200 mg/mL; M7, ESM Table S2) [34], the signal intensity of peptide ions increased significantly in both TOF and IMS modes (Fig. 2). The signal intensities of most peptide ions were in the same order of magnitude as when using the matrix CHCA. Most notably, the signal intensity of the largest peptide ion (*m/z* 3257.62) was one order of magnitude higher compared with that of the matrix CHCA, and the signal was visible in all recorded mass spectra. The same effects were observed in IMS mode. In the drift plot of the IMS measurements, the diagonal line of the doubly charged ions was more intense compared with the measurements using the matrix CHCA (Fig. 2B). Furthermore, a new diagonal line appeared in the drift plots, corresponding to triply charged peptide ions. The doubly charged peptide ion at *m/z* 1629.81 was detected in all mass spectra with a signal intensity two to three orders of magnitudes higher compared to CHCA mass spectra. Due to their higher signal intensities, the signal-to-noise ratio of the doubly charged peptides increased by a factor of 1.6 to 4. We suggest that the high concentration of DHB results in more

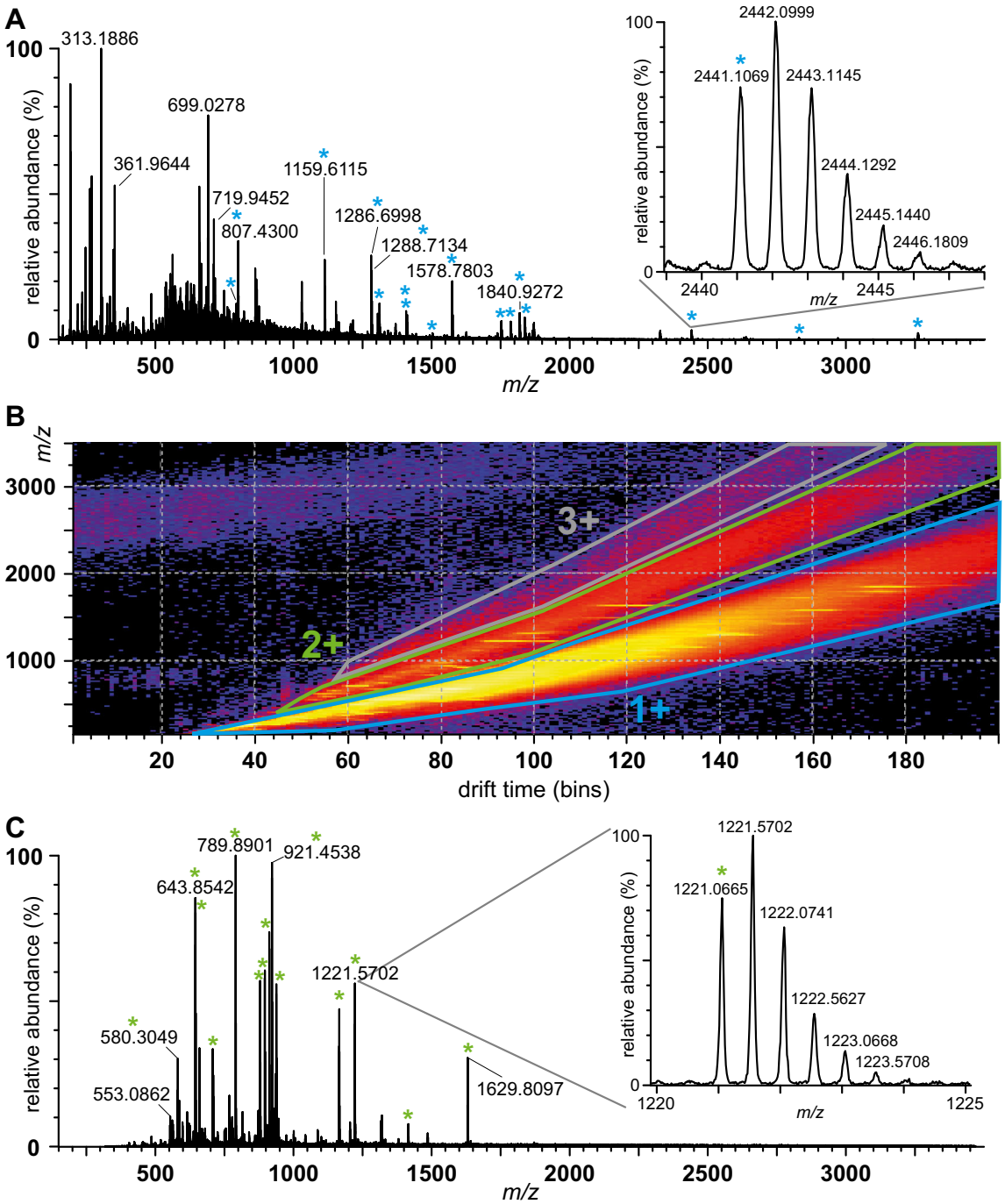

Fig. 2 **A** Mass spectrum of yeast enolase I tryptic digest in TOF mode obtained by using the matrix DHB (M7, ESM Table S2). Peaks marked with blue asterisk were matched to $[M + H]^+$ enolase peptides. **B** Drift plot of the same sample acquired in IMS mode using DHB matrix (M7). Three diagonal lines can be easily distinguished, corresponding to ions with one to three charges. **C** Mass spectrum obtained after extraction of the drift region of doubly charged ions (green border). Peaks marked with green asterisk were matched to $[M + 2H]^{2+}$ enolase peptides

needle-like matrix crystals, which are known to yield the highest amounts of peptide ions. Next to the different morphologies of the higher concentrated DHB matrix, the change in the analyte-to-matrix ratio might be responsible for the increased signal intensity. Due to the excellent performance of the DHB matrix formulation M7, we used this matrix formulation for the tandem MS experiments in TOF and IMS mode.

Tandem MS experiments

Nine enolase peptide ions were selected for further evaluation (ESM Table S4). The quadrupole of the Q-TOF mass spectrometer was used to isolate the precursor ion. We compared the protein identification using CID tandem MS data acquired in the TOF mode (ion mobility disabled,

ions fly through an evacuated IMS cell, ESM Fig. S5A) and tandem MS data acquired in IMS mode (IMS separation enabled, fragmentation after IMS separation in the second collision cell of the instrument, ESM Fig. S5B). In IMS mode, this results in distinct vertical ion series in the drift plots, as the fragment ions possess the same drift time as their precursor ion (Fig. 3). When doubly charged ions are fragmented, the *m/z* value of the fragment ions can be higher than the *m/z* value of the doubly charged precursor ion. Therefore, the drift time of the doubly charged precursor ion is straightforwardly identified in the drift plot as the vertical ion

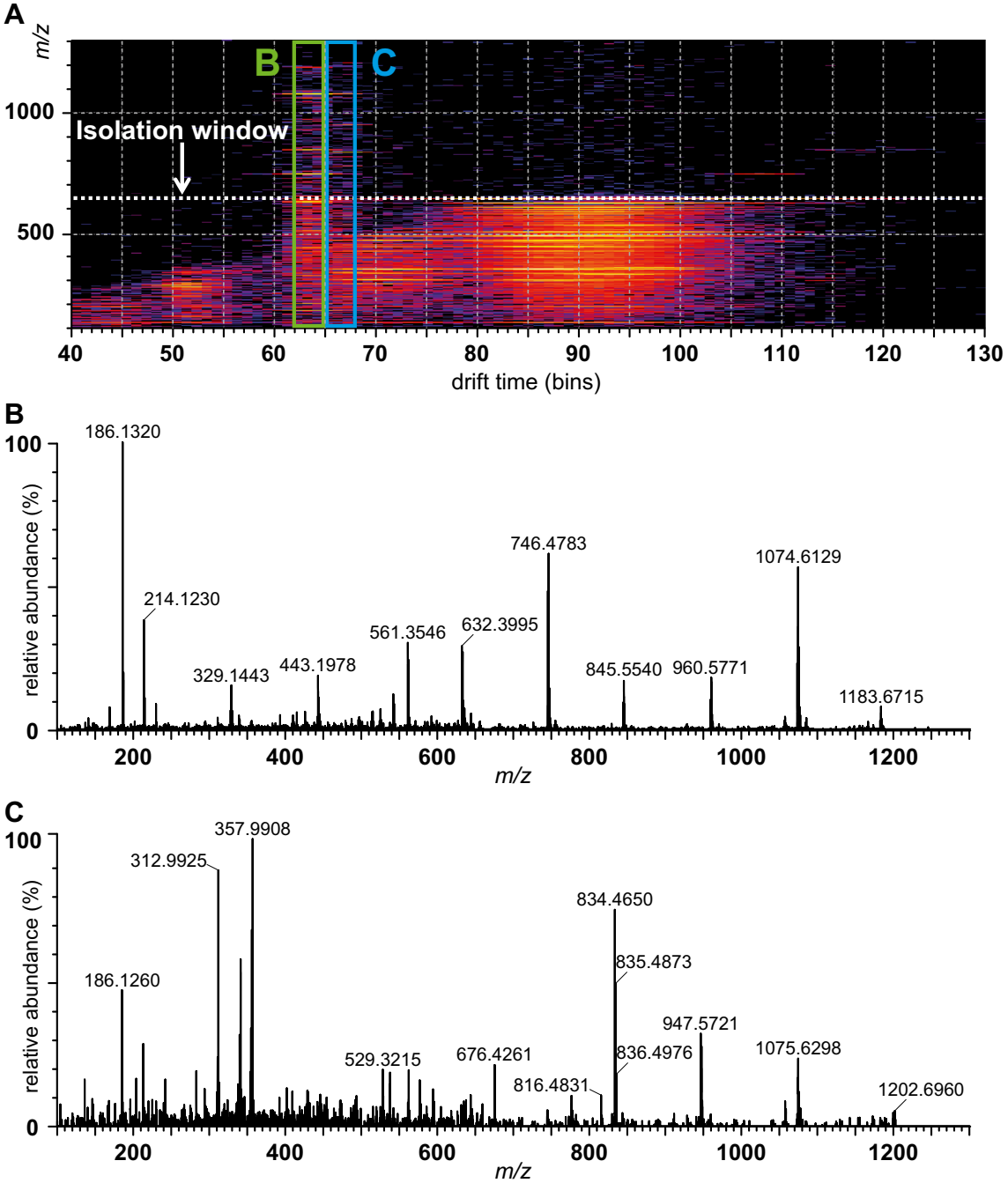

Fig. 3 **A** Drift plot obtained from an IMS-MSMS experiment (compare Fig. S5). The isolation window (*m/z* 643.86, 4 Da width) is marked as a horizontal dotted line. Fragment ions generated from doubly charged precursors can be easily identified by vertical trends and the presence of signals above the *m/z* value of the isolation window. Due to the overlap of the almost isobaric doubly charged peptides VNQIGTLSESIK (*m/z* 644.86) and NVNDVIAPAFVK (*m/z* 643.86, compare Fig. 1B1), both peptides are cofragmented during this tandem MS experiment. **B** Fragment ion mass spectrum obtained by the extraction of the bins 63 and 64 from the drift plot. **C** Fragment ion mass spectrum obtained by the extraction of the bins 66 and 67 from the drift plot

series of the fragment ions extends above the *m/z* value of the precursor ion.

The Mascot database search using the tandem MS data acquired from singly charged precursor ions identified yeast enolase I with a score of 570 (ESM Table S5). Using the IMS tandem MS data from doubly charged precursor ions, however, the Mascot score for the identification of enolase increased to 848 (ESM Table S5). As reported by Cramer and Corless [19], the fragmentation of doubly charged peptide ions yielded more y-type ions compared with that of their singly charged counterparts. IMS enables the separation of peptides with low differences in their *m/z* value due to their different collisional cross sections, resulting in distinct fragment mass spectra of both precursor ions (Fig. 3B, C). Additionally, IMS separation reduces significantly the amount of fragment ions originating from co-isolated singly charged matrix ions or other (almost) isobaric ions within the isolation window of the quadrupole. Thereby, tandem mass spectra acquired in the IMS mode exhibit a significantly reduced amount of noise and chimeric fragment ions. This results in higher identification scores, as the majority of peaks with high signal intensity are matched to fragment ions of the peptide ion. This can be observed with the fragment ion spectra of the peptides VNQIGTLSESIK (Fig. 4) and NVNDVIAPAFVK (ESM Fig. S6). Using the TOF mode,

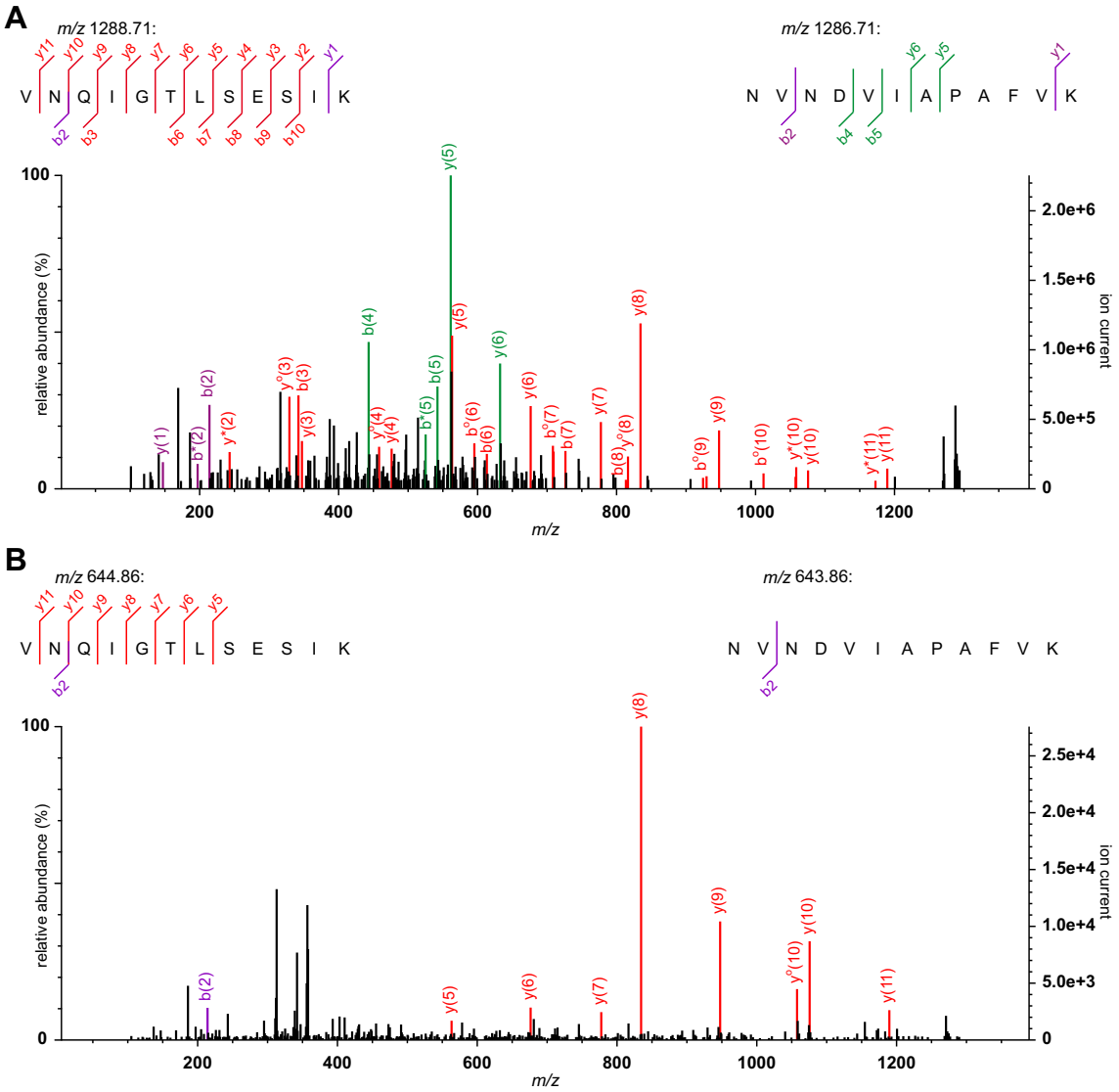

Fig. 4 **A** Cofragmented mass spectrum of the singly protonated precursor ion at *m/z* 1288.71. Next to a high number of fragment ions matched to peptide VNQIGTLSESIK, other high intense peaks (including the base peak) were matched to peptide NVNDVIAPAFVK (*m/z* 1286.71). Both peptides were within the isolation window of the quadrupole, resulting in a chimeric fragment ion mass spectrum. **B** Fragment ion mass spectrum obtained in IMS mode from the doubly charged precursor ion *m/z* 644.86 (compare Fig. 3). Because of the IMS separation, fragment ions can be matched almost exclusively to the peptide VNQIGTLSESIK, resulting in a more reliable identification of the peptide

both peptides are isolated in the isolation window of the quadrupole yielding chimeric tandem mass spectra. The fragment spectrum generated from the precursor ion at *m/z* 1288.71 (VNQIGTLSESIK) is an example of such a chimeric fragment ion mass spectrum—the complete y-ion series of the peptide VNQIGTLSESIK was identified by Mascot; however, the base peak and several other peaks of high intensity were not matched to fragment ions of this peptide. However, these peaks can be assigned to three b-ions and two y-ions of the peptide NVNDVIAPAFVK (*m/z* 1286.71; Fig. 4A).

The IMS mode enables a more confident peptide identification by Mascot. The fragment ion mass spectra generated from the precursor ion at *m/z* 644.86 (VNQIGTLSESIK) yielded only peaks matched to fragment ions of the peptide VNQIGTLSESIK (Fig. 4B), and only the b_2-ion can be matched to the peptide NVNDVIAPAFVK. However, this is most likely a coincidence, as the b_2-ions of both peptides contain the amino acids valine and asparagine. Thus, when using IMS, it is possible to reduce the generation of chimeric fragment ion mass spectra and enable an unambiguous identification of peptide sequences.

In addition, we observed that with increasing *m/z* value of the doubly charged precursor ion, the fragment ion mass spectra yielded even higher Mascot scores. Tryptic peptides carry the proton and therefore the charge most likely on the basic *N*-terminus and the basic side chain of the *C*-terminal K or R. The formation of two fragment ions from a doubly charged precursor ion might be more likely with increasing length of the peptide and thereby increasing mass. In contrast, singly charged peptide ions only yield one fragment ion and a neutral fragment. E.g., the Mascot score of the largest singly

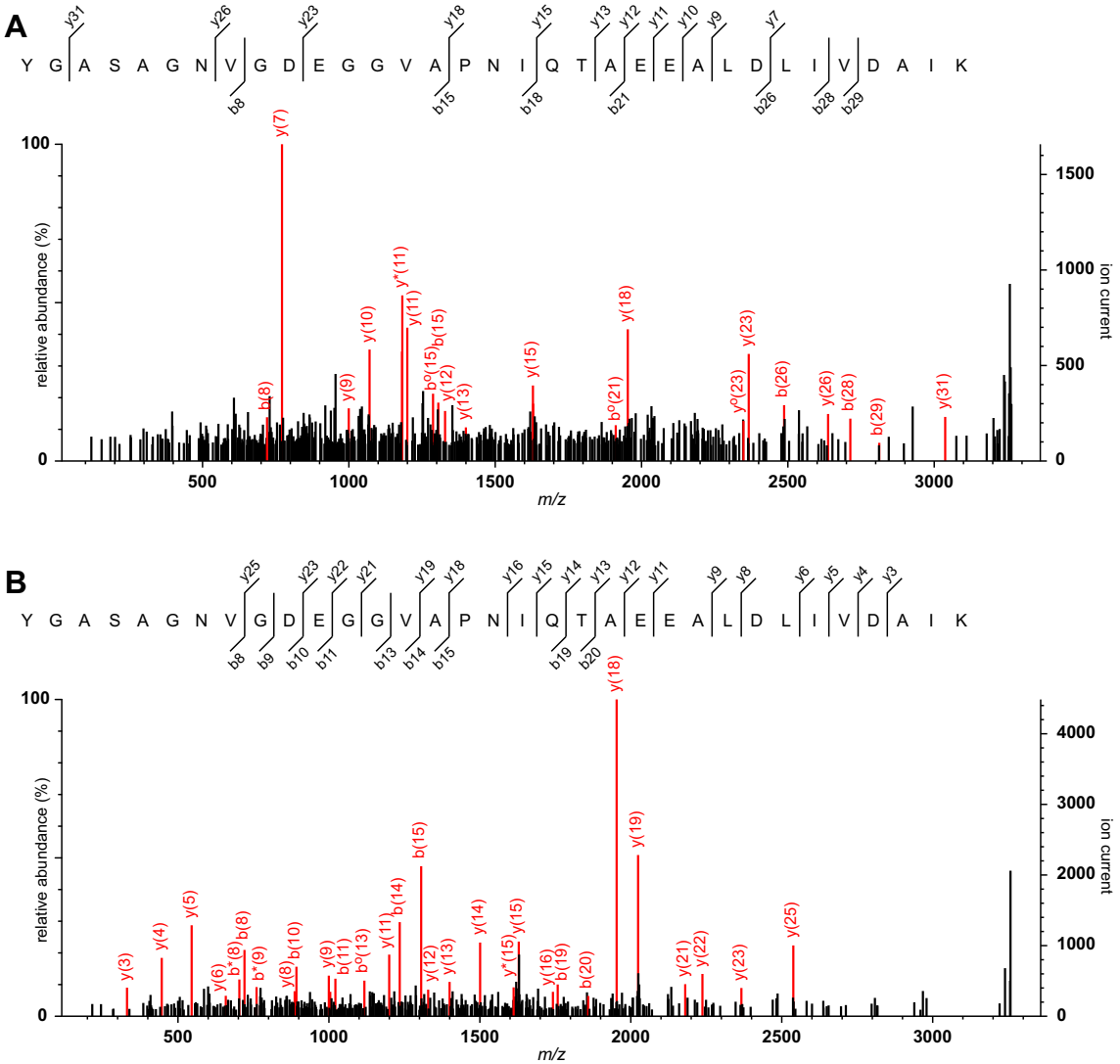

Fig. 5 **A** Fragment ion mass spectrum of the singly charged precursor ion at *m/z* 3257.62. **B** Fragment ion mass spectrum of the doubly charged precursor ion *m/z* 1629.81 obtained in IMS mode. The fragment ion mass spectrum of the doubly charged ion contains a higher number of fragment ions compared with the fragment ion mass spectrum generated from the singly charged precursor ion

protonated enolase peptide observed at *m/z* 3257.62 was 14 (Fig. 5A). It is noteworthy that when using the fragment ion spectrum of the doubly protonated precursor of the same peptide at *m/z* 1629.81, a Mascot peptide score of 107 was obtained (Fig. 5B). This value strongly is significantly higher than the Mascot peptide score for a confident identification of a peptide (> 40).

Comparing the Mascot identification of the peptides with shorter sequences (< 15 amino acids) using singly and doubly charged precursor ions, Mascot peptide scores are very similar. However, fragment ion mass spectra generated of singly charged precursor ions contain more fragment ions matched to the peptide sequence, including fragment ions with water and/or ammonia loss. In contrast, fragment ion mass spectra generated from doubly charged precursor ions contain fewer fragment ions matched to the peptide sequence; however, the signal-to-noise ratio of these fragment ions is higher due to the IMS cleanup. The lower noise level in the IMS data compensates the lower amount of fragment ions and enables a peptide identification with high confidence (Fig. 4 and ESM Fig. S6).

Analysis of ene reductase tryptic digest

Using the optimized setup, we analyzed a tryptic *in-solution* digest of the *N*-terminally his-tagged ene reductase from *G. oxydans* as an example for a versatile biocatalyst having been applied already for a range of synthetic applications [32,

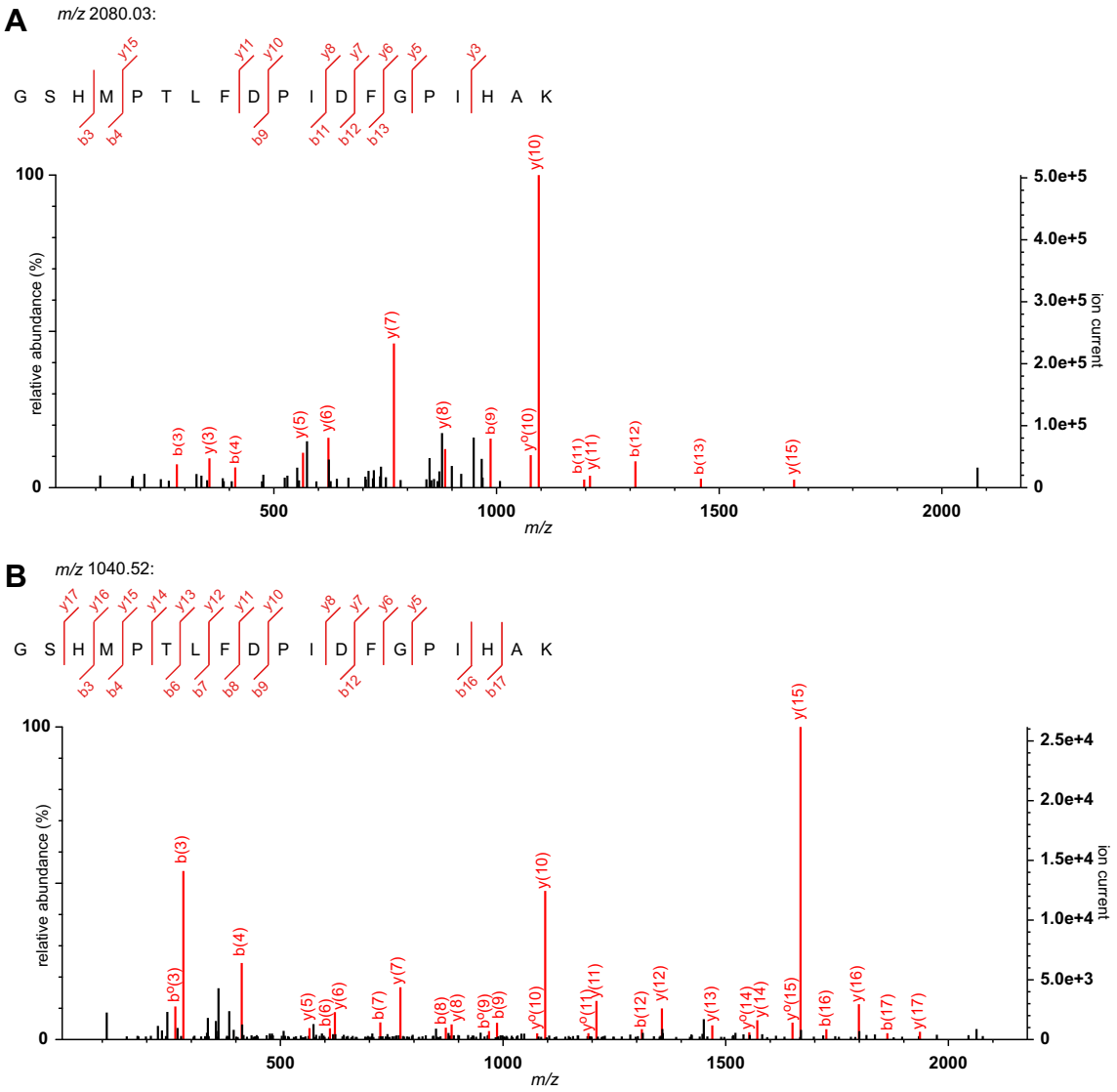

Fig. 6 Tryptic digest of *N*-terminally his-tagged ene reductase from *G. oxydans*: **A** Fragment ion mass spectrum of the singly charged precursor ion at *m/z* 2080.03. **B** Fragment ion mass spectrum of the doubly charged precursor ion *m/z* 1040.52 obtained in IMS mode. The fragment ion mass spectrum of the doubly charged ion contains a higher number of fragment ions compared with the fragment ion mass spectrum generated from the singly charged precursor ion

35–39] in the field of enzymatic C=C double bond reductions (ESM Fig. S7). We generated fragment ion spectra in TOF mode (singly charged precursor ions; Fig. 6A, ESM Figs. S8A and S9A) and in IMS mode (doubly charged precursor ions, Fig. 6B, ESM Figs. S8B and S9B). The protein was identified by Mascot database search with a score of 540 (TOF mode) and 870 (IMS mode). Again, peptide scores of short peptides were similar in both settings, whereas peptides of at least 15-amino acid length yielded higher scores, when fragment ion mass spectra of doubly charged precursors were used for the database search.

Conclusion

The use of ion mobility separation of tryptic peptides in combination with the matrix 2,5-dihydroxybenzoic acid yielded multiply charged peptides in MALDI experiments and enabled an efficient selection of doubly charged peptide ions. These ions can be subjected to CID fragmentation post-IMS, and the generated fragment ion mass spectra can be effectively used for protein identification by PFF. With increasing length of the peptides, doubly protonated precursors yielded significantly higher numbers of fragments compared to the fragment ion mass spectra generated from singly charged precursor ions. Compared with PFF from singly charged peptide ions, Mascot scoring was significantly increased for the doubly charged peptide approach. Therefore, identification of proteins, as shown with enolase I from *S. cerevisiae* and ene reductase from *G. oxydans*, is more reliable in MALDI. This approach opens up a perspective towards automated drift time-dependent fragment spectrum extraction methods of complex peptide mixtures comparable to the UDMSe approach [28], and new identification tools in protein analytics.

Acknowledgements The authors thank T. Winkler for the preparation of ene reductase.

Funding information J.S. and H.G. received generous support from the German Research Foundation (DFG; grant number: INST 215/484-1 FUGG).

Compliance with ethical standards

Conflict of interest Jens Sproß and Harald Gröger declare no conflict of interest. Alexander Muck is an employee of Waters Corp.

References

1. Aebersold R, Mann M. Mass spectrometry-based proteomics. Nature. 2003;422:198–207.
2. Sinz A. Chemical cross-linking and mass spectrometry to map three-dimensional protein structures and protein-protein interactions. Mass Spectrom Rev. 2006;25:663–82.
3. Mallick P, Kuster B. Proteomics: a pragmatic perspective. Nat Biotechnol. 2010;28:695–709.
4. Shevchenko A, Tomas H, Havli J, Olsen JV, Mann M. In-gel digestion for mass spectrometric characterization of proteins and proteomes. Nat Protoc. 2007;1:2856–60.
5. Jaskolla TW, Karas M. Compelling evidence for lucky survivor and gas phase protonation: the unified MALDI analyte protonation mechanism. J Am Soc Mass Spectrom. 2011;22:976–88.
6. Alves S, Fournier F, Afonso C, Wind F, Tabet JC. Gas-phase ionization/desolvation processes and their effect on protein charge state distribution under matrix-assisted laser desorption/ionization conditions. Eur J Mass Spectrom. 2006;12:369–83.
7. Kononikhin AS, Nikolaev EN, Frankevich V, Zenobi R. Letter: multiply charged ions in matrix-assisted laser desorption/ionization generated from electrosprayed sample layers. Eur J Mass Spectrom. 2005;11:257–9.
8. Liu ZL, Schey KL. Fragmentation of multiply-charged intact protein ions using MALDI TOF-TOF mass spectrometry. J Am Soc Mass Spectrom. 2008;19:231–8.
9. Koch A, Schnapp A, Soltwisch J, Dreisewerd K. Generation of multiply charged peptides and proteins from glycerol-based matrices using lasers with ultraviolet, visible and near-infrared wavelengths and an atmospheric pressure ion source. Int J Mass Spectrom. 2017;416:61–70.
10. König S, Kollas O, Dreisewerd K. Generation of highly charged peptide and protein ions by atmospheric pressure matrix-assisted infrared laser desorption/ionization ion trap mass spectrometry. Anal Chem. 2007;79:5484–8.
11. Leisner A, Rohlfing A, Berkenkamp S, Hillenkamp F, Dreisewerd K. Infrared laser post-ionization of large biomolecules from an IR-MALD(I) plume. J Am Soc Mass Spectrom. 2004;15:934–41.
12. Ryumin P, Brown J, Morris M, Cramer R. Investigation and optimization of parameters affecting the multiply charged ion yield in AP-MALDI MS. Methods. 2016;104:11–20.
13. Ryumin P, Brown J, Morris M, Cramer R. Protein identification using a nanoUHPLC-AP-MALDI MS/MS workflow with CID of multiply charged proteolytic peptides. Int J Mass Spectrom. 2017;416:20–8.
14. Cramer R, Pirkl A, Hillenkamp F, Dreisewerd K. Liquid AP-UV-MALDI enables stable ion yields of multiply charged peptide and protein ions for sensitive analysis by mass spectrometry. Angew Chem Int Ed. 2013;52:2364–7.
15. Jaskolla TW, Lehmann W-D, Karas M. 4-Chloro-alpha-cyanocinnamic acid is an advanced, rationally designed MALDI matrix. PNAS. 2008;105:12200–5.
16. Jaskolla TW, Papasotiriou DG, Karas M. Comparison between the matrices alpha-cyano-4-hydroxycinnamic acid and 4-chloro-alpha-cyanocinnamic acid for trypsin, chymotrypsin, and pepsin digestions by MALDI-TOF mass spectrometry. J Proteome Res. 2009;8:3588–97.
17. Soltwisch J, Jaskolla TW, Hillenkamp F, Karas M, Dreisewerd K. Ion yields in UV-MALDI mass spectrometry as a function of excitation laser wavelength and optical and physico-chemical properties of classical and halogen-substituted MALDI matrixes. Anal Chem. 2012;84:6567–76.
18. Wiegelmann M, Soltwisch J, Jaskolla TW, Dreisewerd K. Matching the laser wavelength to the absorption properties of matrices increases the ion yield in UV-MALDI mass spectrometry. Anal Bioanal Chem. 2013;405:6925–32.
19. Cramer R, Corless S. The nature of collision-induced dissociation processes of doubly protonated peptides: comparative study for the future use of matrix-assisted laser desorption/ionization on a hybrid quadrupole time-of-flight mass spectrometer in proteomics. Rapid Commun Mass Spectrom. 2001;15:2058–66.
20. Paizs B, Suhai S. Fragmentation pathways of protonated peptides. Mass Spectrom Rev. 2005;24:508–48.

21. Cumeras R, Figueras E, Davis CE, Baumbach JI, Gràcia I. Review on ion mobility spectrometry. Part 1: current instrumentation. Analyst. 2015;140:1376–90.
22. Bohrer BC, Merenbloom SI, Koeniger SL, Hilderbrand AE, Clemmer DE. Biomolecule analysis by ion mobility spectrometry. Annu Rev Anal Chem (Palo Alto, Calif). 2008;1:293–327.
23. Seo J, Hoffmann W, Warnke S, Bowers MT, Pagel K, von Helden G. Retention of native protein structures in the absence of solvent: a coupled ion mobility and spectroscopic study. Angew Chem Int Ed. 2016;55:14173–6.
24. Pagel K, Harvey DJ. Ion mobility-mass spectrometry of complex carbohydrates: collision cross sections of sodiated N-linked glycans. Anal Chem. 2013;85:5138–45.
25. Hofmann J, Hahm HS, Seeberger PH, Pagel K. Identification of carbohydrate anomers using ion mobility–mass spectrometry. Nature. 2015;526:241–4.
26. Stauber J, MacAleese L, Franck J, Claude E, Snel M, Kaletas BK, et al. On-tissue protein identification and imaging by MALDI-ion mobility mass spectrometry. J Am Soc Mass Spectrom. 2010;21:338–47.
27. Inutan ED, Wager-Miller J, Narayan SB, Mackie K, Trimpin S. The potential for clinical applications using a new ionization method combined with ion mobility spectrometry-mass spectrometry. Int J Ion Mobil Spectrom. 2013;16:145–59.
28. Distler U, Kuharev J, Navarro P, Tenzer S. Label-free quantification in ion mobility-enhanced data-independent acquisition proteomics. Nat Protoc. 2016;11:795–812.
29. Pringle SD, Giles K, Wildgoose JL, Williams JP, Slade SE, Thalassinos K, et al. An investigation of the mobility separation of some peptide and protein ions using a new hybrid quadrupole/travelling wave IMS/oa-ToF instrument. Int J Mass Spectrom. 2007;261:1–12.
30. Henzel WJ, Billeci TM, Stults JT, Wong SC, Grimley C, Watanabe C. Identifying proteins from two-dimensional gels by molecular mass searching of peptide fragments in protein sequence databases. Proc Natl Acad Sci U S A. 1993;90:5011–5.
31. Mann M, Højrup P, Roepstorff P. Use of mass spectrometric molecular weight information to identify proteins in sequence databases. Biol Mass Spectrom. 1993;22:338–45.
32. Richter N, Gröger H, Hummel W. Asymmetric reduction of activated alkenes using an enoate reductase from Gluconobacter oxydans. Appl Microbiol Biotechnol. 2011;89:79–89.
33. Sladkova K, Houska J, Havel J. Laser desorption ionization of red phosphorus clusters and their use for mass calibration in time-of-flight mass spectrometry. Rapid Commun Mass Spectrom. 2009;23:3114–8.
34. Inutan ED, Wang BX, Trimpin S. Commercial intermediate pressure MALDI ion mobility spectrometry mass spectrometer capable of producing highly charged laserspray ionization ions. Anal Chem. 2011;83:678–84.
35. Kraußer M, Winkler T, Richter N, Dommer S, Fingerhut A, Hummel W, et al. Combination of C=C bond formation by Wittig reaction and enzymatic C=C bond reduction in a one-pot process in water. ChemCatChem. 2011;3:293–6.
36. Burda E, Reß T, Winkler T, Giese C, Kostrov X, Huber T, et al. Highly enantioselective reduction of α-methylated nitroalkenes. Angew Chem Int Ed. 2013;52:9323–6.
37. Reß T, Hummel W, Hanlon SP, Iding H, Gröger H. The organic-synthetic potential of recombinant ene reductases: substrate-scope evaluation and process optimization. ChemCatChem. 2015;7:1302–11.
38. Biermann M, Gruß H, Hummel W, Gröger H. Guerbet alcohols: from processes under harsh conditions to synthesis at room temperature under ambient pressure. ChemCatChem. 2016;8:895–9.
39. Biermann M, Bakonyi D, Hummel W, Gröger H. Design of recombinant whole-cell catalysts for double reduction of C=C and C=O bonds in enals and application in the synthesis of Guerbet alcohols as industrial bulk chemicals for lubricants. Green Chem. 2017;19:405–10.